Environmentally Benign Solution-Based Procedure for the Fabrication of Metal Oxide Coatings on Metallic Pigments

Thorsten Bies,[a] Rudolf C. Hoffmann,[a] Matthias Stöter,[b] Adalbert Huber,[b] and Jörg J. Schneider*[a]

Aluminum pigments were coated with Fe_2O_3 and CuO by solution-based thermal decomposition of the urea nitrate compounds hexakisureairon(III)nitrate and tetrakisureacopper(II) nitrate. The deposition process was optimized to obtain homogeneously coated aluminum pigments. The growth of the surface coatings was controlled by investigation with scanning electron microscopy, energy dispersive X-ray spectroscopy and static light scattering as well as infrared, X-ray diffraction and thermogravimetric analysis. The iron precursor showed an incomplete decomposition in solution, incorporating traces of urea molecules inside the coatings while the copper precursor showed complete dissociation accompanied by in situ formation of amine complexes. The amount of organic residues resulting from ligand fragments in the final oxide coatings could be reduced to 22% for the iron oxide and 12% for the copper oxide by further temperature treatment in solution (259 °C). Colorimetric investigations of the obtained pigments revealed an excellent hiding power, outperforming the pigments used in current state-of-the-art formulations.

1. Introduction

Metal oxides have a long history as coloring agents in the form of absorption pigments.[1–3] In the past decades, their application has been extended, as they find usage in the formation of special effect pigments, which are based on a multi-layer design of materials with varying refractive indices.[4,5] If the core is a metal effect pigment, e.g. aluminum, these pigments form a mirror-like surface in a varnish and show targeted reflection of light, leading to varying appearances when observed from different angles ("flop-effect"). In order to obtain brilliant films, it is important to synthesize homogeneous materials with most perfect and smooth surfaces, as irregularities on the surface like cracks or roughness lead to undirected reflection resulting in decreasing luster (Figure 1, right).[6] Typically commercially used aluminum base pigments which are widely used as substrates for oxide coatings are the so called "silverdollar pigments", which have a thickness of about 150–300 nm.[7] Aluminum pigments accessible by physical vapor deposition (PVD) show a thickness of only 1–50 nm.[7] These types of pigments are used e.g. in cosmetics, automotive coatings and secure document applications.[7] Owing to their multi-layer design, special effect pigments like the oxide coated aluminum pigments, show interesting optical phenomena. When they are irradiated, the incoming light is diffracted at every layer into a reflected and a transmitted part. Due to the resulting varying path difference between the light waves, constructive and destructive interference occur so that an angle dependent color change can be observed (Figure 1). The main parameters influencing these effects are the refractive index of the dielectric layer and its size as these parameters explicitly define the path difference, meaning that by defined choice of material and coating thickness the properties and the appearance of the pigment can be adjusted as desired.[4,7,8] Materials of choice for the layer formation are metal oxides with high refractive indices like TiO_2,[9–11] Cr_2O_3[12,13] and Co_2O_3[14] or mixed oxides like $Bi_4Ti_3O_{12}$ and $CoAl_2O_4$.[15,16] Due to its absorption properties, an oxide widely used for red and gold colored effect pigments is Fe_2O_3.[17,18]

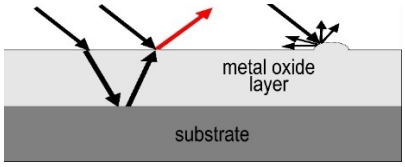

Figure 1. Schematic diagram showing interference-induced color change in a multi-layer thin film arrangement. Diffuse reflection of light due to an inhomogeneous surface is demonstrated on the right.

The most common route for the coating of aluminum pigments with metal oxides is the sol-gel process which is based on hydrolysis of metal salts (mainly alkoxides) in presence of the substrate to be coated. In this process pH and temperature must be controlled precisely to obtain a homogeneous

[a] T. Bies, Dr. R. C. Hoffmann, Prof. Dr. J. J. Schneider
Department of Chemistry
Eduard-Zintl-Institut für Anorganische und Physikalische Chemie
Technische Universität Darmstadt
Alarich-Weiss-Straße 12
64287 Darmstadt (Germany)
E-mail: joerg.schneider@tu-darmstadt.de
[b] Dr. M. Stöter, Dr. A. Huber
Schlenk Metallic Pigments GmbH
Barnsdorfer Hauptstraße 5
91154 Roth (Germany)

Supporting information for this article is available on the WWW under https://doi.org/10.1002/open.202000223

film in desired thickness and smoothness, which is dried and finally calcined in order to produce the desired oxide coating.[19–21] As an example, an oxidic layer can be deposited by slow addition of a 3% $FeCl_3$ solution into an aqueous dispersion containing the substrates at 75 °C and pH 3. The pH is kept constant by simultaneous addition of NaOH. The coating thickness can be controlled by the amount of iron salt added.[20] One major drawback of this procedure is that an aluminum pigment used as substrate isn't stable under the conditions required for the precipitation, as it dissolves in both acidic and basic media.[22] Therefore, it must be encapsulated in a protective shell, normally SiO_2, prior to the desired metal oxide coating.[7,23–26] This additional layer renders the process more difficult and is disadvantageous from a coloristic point of view, as it causes the hiding power to decrease due to the higher pigment thickness.[27,28] An alternative approach is based on a variation of the chemical vapor deposition (CVD) technique, where a metal oxide precursor e.g. $Fe(CO)_5$, is fed into a fluidized-bed reactor together with the base pigment to be coated and heated under an inert atmosphere. Through controlled addition of oxygen or water as oxidizing agents the precursor can be decomposed in a controlled manner (Eq. 1), forming a homogeneous coating.[29]

$$2\ Fe(CO)_5 + Al + 1.5\ O_2 \xrightarrow{\Delta,\ N_2} Fe_2O_3/Al_{core} + 5\ CO_2 \quad (1)$$

Despite the good process control and the unnecessary protective layer, there are still some downsides of this process as the use of the precursor $Fe(CO)_5$ generates severe safety issues.[29,30] A further limitation is that ultrathin PVD pigments are difficult to be completely fluidized owing to their high surface which leads to agglomeration. It is therefore highly desirable to overcome these current restrictions and to devise a process which allows to generate even thinner pigments e.g. resulting in improved hiding power.

The aim of this work is to develop a synthetic approach for the deposition of optically active metal oxide based thin films on aluminum metal substrates that overcomes the drawbacks of the established procedures described above. For the purpose of reducing the processing effort and of preventing aluminum corrosion forced by working in an acidic or basic solvent medium, a new coating procedure based on the thermal decomposition of a molecular single-source metal precursor complex in an organic solvent is developed. This allows to control the coating thickness and the optical parameters by variation of the initial molecular precursor concentration. This procedure also allows for the first time the direct coating of ultrathin pigments e.g. obtained by PVD from solution without any protective layer to shield the bare metal surface of the aluminum base pigments towards corrosion. This new solution-based approach could allow to reach better hiding power of the coatings as compared to currently available established special effect pigments based on a composite composition of a metal substrate and an oxide. From a technological viewpoint such a suitable precursor complex must fulfill certain requirements to be an appropriate candidate. It should be nontoxic, stable under ambient conditions and most easy to synthesize in order to be interesting and easy to apply under a potential large-scale process. Furthermore, it should decompose at relatively low temperatures with preferably low amounts of organic residues. A promising group of such compounds possessing all the desired characteristics are urea nitrate complexes. Urea nitrate is a well-known compound that combines an oxidizing agent (nitrate) with a fuel (urea), making it a promising substance for the combustion synthesis of metal oxides under controlled conditions (Figure 2).[31] In this type of reactions, the processing temperature needed for obtaining a metal oxide can be drastically reduced e.g. compared to the widely used sol-gel type approach.[32] The oxidizer-fuel combination leads to a strong exothermic decomposition when being exposed to a thermal treatment. Thereby, it provides the overall energy for the oxide formation and reduces the additional external energy effort needed. This approach has been proven suitable for the low temperature synthesis (200–300 °C) of metal oxide semiconductors starting from metal nitrate and acetylacetone.[32]

Furthermore, urea complexes are very versatile and have been reported for a large variety of metals[33–40] thus making a large group of metal oxides potentially accessible. It has already been shown that indium, gallium and zinc oxides can be deposited by use of these compounds as thin films by a spin coating technique for thin film transistor applications.[31] In this work we will devise a new route to obtain homogeneous metal oxide coatings on thin physical vapor deposited metal effect pigments, especially aluminum, in solution by use of the thermal transformation of urea nitrate complexes resulting in highly dense thin and smooth metal coatings.

2. Results and Discussion

2.1. Metal Oxide Precursor Synthesis and Characterization

Precursor compounds $[Fe(urea)_6](NO_3)_3$ (**1**) and $[Cu(urea)_4](NO_3)_2$ (**2**) were synthesized by mixing stoichiometric amounts of metal nitrates and urea in ethanol (**1**) or n-butanol (**2**) (Scheme 1)(all spectroscopic data are given in the SI). Due to the coordination, the CO stretching vibration shifted to 1625 cm^{-1} in both complexes compared to 1675 cm^{-1} in uncoordinated urea. On the other hand, the CN stretching vibration showed a hypsochromic shift from 1459 cm^{-1} in uncoordinated urea to

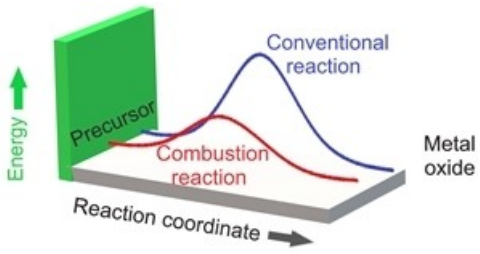

Figure 2. Schematic overview of the energy profile of a conventional thermal pathway (blue) compared with an internal combustion reaction for the metal oxide synthesis starting from a molecular precursor.

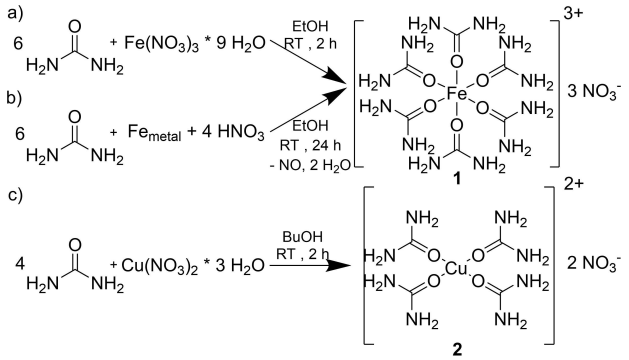

Scheme 1. Reaction scheme of formation of the iron urea coordination compound **1** using iron nitrate (a) or directly metallic iron (b). Formation of the copper urea compound **2** using copper nitrate and urea (c).

1504 cm^{-1} (**1**) and to 1508 cm^{-1} (**2**).[41–43] In an alternative approach we have found that **1** is also accessible in a direct reaction using elemental metallic iron, nitric acid and urea, giving rise to the possibility of implementing that approach into an even more eco-friendly procedure.

Thermogravimetric studies allow to control the purity of the obtained precursors and to evaluate their thermal behavior in the solid state (Figure 3a). This allows to elucidate the thermal transformation and precipitation process of the oxide films. Compound **1** decomposes in one steep step in the temperature range between 200–250 °C.[43,44]

The thermal decomposition of compound **2** is described herein for the first time. **2** was found to decompose in three main steps (Figure 3a). First, from 115 °C to 160 °C a mass loss of 4% is found, followed by a second step from 160 °C to 300 °C which generates 64% of the observed mass loss. In the last step, up to 415 °C 14% of the remaining mass loss is detected. Figure 3 shows the ion currents of the corresponding fragments as detected by TG-MS (b), the Gram-Schmidt intensities during the decomposition process (c) and the IR spectra measured at the maxima (d). The Gram-Schmidt curve shows that the gas evolving in the first step consists mainly of isocyanic acid (HNCO = 2283 and 2252 cm^{-1}), which indicates a beginning decomposition of the urea ligand. This is followed by decomposition of urea nitrate which show signals corresponding to HNCO (2283, 2252, 3535 cm^{-1}), N_2O (2243 and 2212 cm^{-1}), CO_2 (2358, 2327, 668 cm^{-1}) and NH_3 (3331, 1625, 966, 930 cm^{-1}).[45] The obtained mass spectra of the evolved gases show the expected signals for the urea decomposition, which are ammonia (m/z^+ 17), water (m/z^+ 18), carbon monoxide/nitrogen (m/z^+ 28), nitric oxide (m/z^+ 30), isocyanic acid (m/z^+ 43), carbon dioxide (m/z^+ 44) and nitrogen dioxide (m/z^+ 46). Peaks observed in the IR spectra at 1599 cm^{-1} could not be assigned unambiguously, however are most likely to be attributed to carboxylic compounds formed also during urea decomposition.

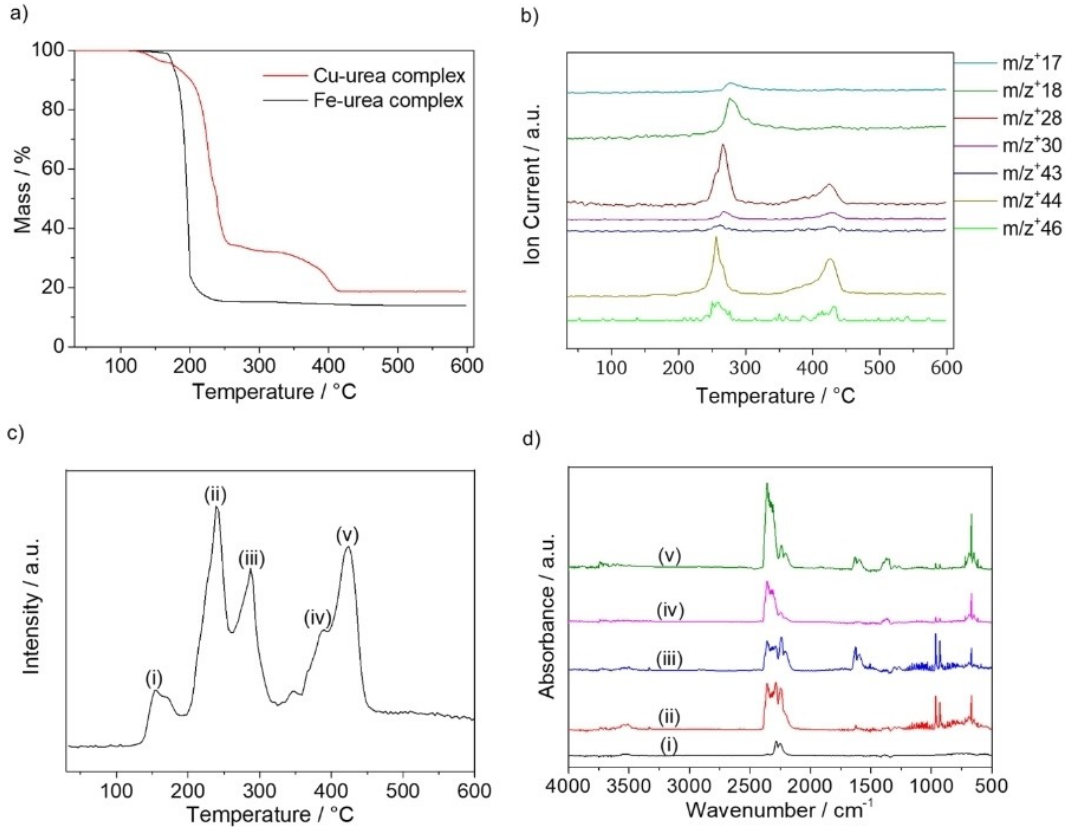

Figure 3. Coupled IR/MS-thermogravimetric mass loss (a) of compounds **1** (black) and **2** (red) under O_2 atmosphere. Shown are ion currents of the mass fragments detected during decomposition of **2** (b); intensity of m/z + 43 multiplied by 10 for enhanced clarity, that of m/z + 46 by 100; and the Gram-Schmidt intensities during decomposition of **2** (c) and the corresponding IR signals of the maxima (d).

This is substantiated by the fact that these bands only appear in maxima iii and v, which are the maxima of the second and third decomposition step observed in the TG. The same could be true for the signal at 1363 cm^{-1}, that is due to some NO containing residue. It could thus be concluded that the decomposition starts with slow decomposition of urea around 140 °C. At about 226 °C, most of the urea and nitrate are released, leaving behind a composite composed of CuO and remaining organic residues. During the decomposition of urea and urea nitrate released isocyanic acid reacts with remaining urea to form biuret, which is known to undergo further polymerization reactions to form compounds like ammelide, ammeline, cyanuric acid and melamine which finally decompose at T > 400 °C.[45–47] These processes are thus well reflected in the observed TG curve.

2.2. Fabrication of Oxide Coated Aluminum-Based Pigments

To obtain a high-quality oxide coated aluminum base pigment, it is important to generate a homogeneous oxide coating on the aluminum base pigment. Therefore, the deposition parameters must be optimized in order to minimize additional surplus oxide precipitation so that a smooth oxide coated pigment not containing any side precipitation on the base pigment's surface is obtained. For the parameter optimization a silverdollar-type base pigment was used, which has a thickness of 150–300 nm (Figure 4a).[7] However, the final optimized coatings were then applied on a physical vapor deposited (PVD) aluminum base pigment with a thickness of only about 1–50 nm (Figure 4b).[7] The diameter of both base pigments is about 22 μm, which is why the PVD base pigments have a strong tendency towards agglomeration when dried due to the higher aspect ratio. Both substrates show homogeneous native surfaces without significant defects.

Any surplus precipitation during the coating process must be avoided since this would increase the amount of diffuse reflected light and therefore directly impair performance parameters like gloss and flop effect. For the evaluation of optimal coating parameters, the pigments were dispersed in a precursor solution in varying ratios and refluxed while monitoring sample composition in certain intervals by EDX which gives the reported medium values and associated standard deviations of the precipitated coatings (Figure 5). Depending on the reaction time, the amount of iron oxide deposition on the aluminum base pigments during decomposition of **1** grows linearly, until a saturation is reached after 100 minutes, indicating that the precipitation is finished at this point (Figure 5a). In comparison, the amount of precipitated copper oxide had already reached a maximum after 30 min and remains constant during ongoing reaction times, indicating a different decomposition mechanism and/or differing reaction kinetics of **2** as compared to **1**. This fact has a major influence on the coating process as a faster precipitation means that the deposition process must be strongly controlled in order to avoid co-precipitation. The main factor influencing the coating quality is the ratio of the amount of transformed precursor and available substrate as it directly influences nucleation taking place on the pigment surface and agglomerate formation of the coated pigments. The EDX analysis of iron oxide coated pigments obtained from decomposition of **1** reveal that the precipitation already takes place at low precursor concentrations compared to **2** but remains constant with only small variations up to a ratio of 1. At this point the resulting Fe/Al ratio starts increasing however accompanied by increasing inhomogeneity of the deposition. At a ratio of about 2.5, this effect further increases significantly. The findings from the EDX investigations are confirmed by the SEM images shown in Figure 6 a-c. At a precursor/aluminum substrate ratio of 0.7 (Figure 6a), the surface looks smooth and no additional particles

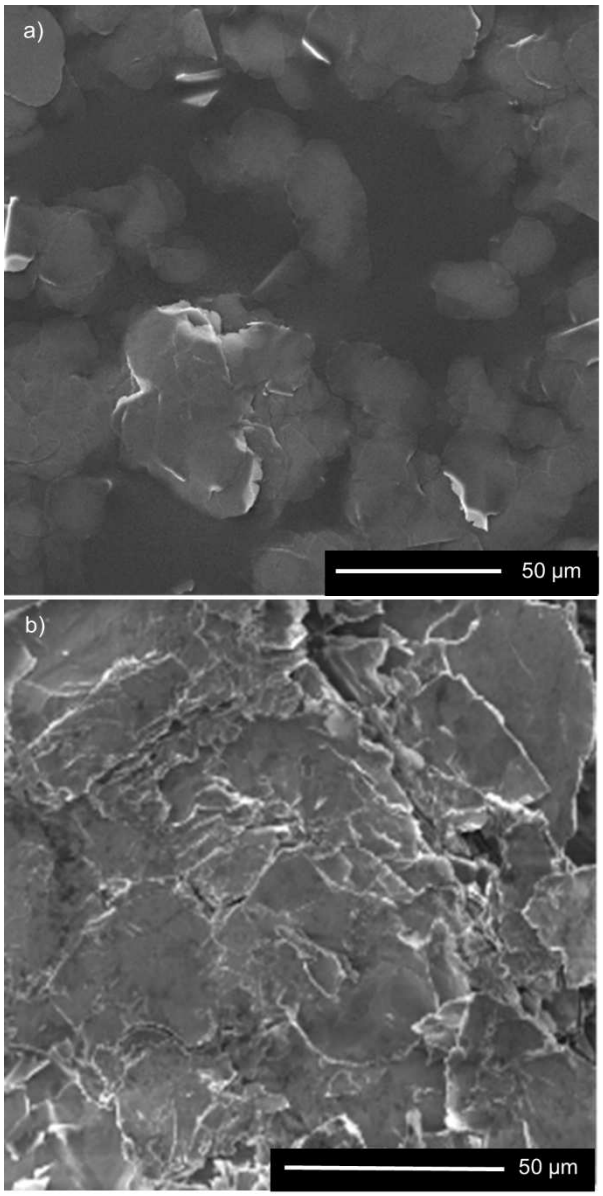

Figure 4. SEM images of a native uncoated silverdollar-type (a) and a native physical vapor deposited aluminum base pigment (b). The silverdollar base pigment particles are visible mainly as isolated particles, while the thinner PVD obtained base pigment particles show a strong surface agglomeration giving rise to a sheet like arrangement.

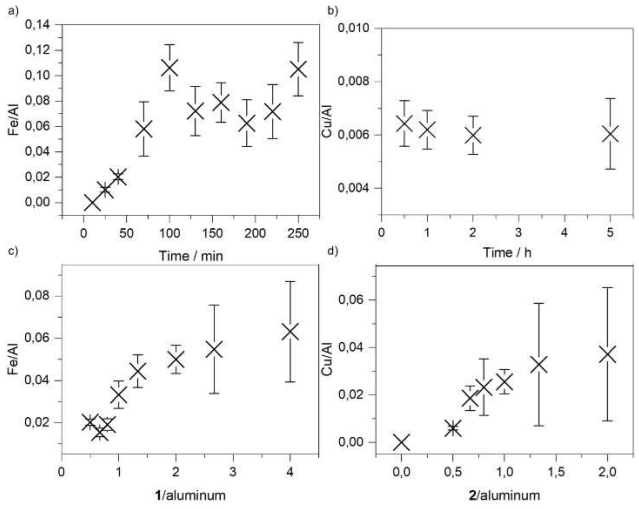

Figure 5. Development of the ratio metal(Fe, Cu)/aluminum vs. deposition time for the decomposition of **1** (a) and **2** (b) and dependence of the ratio precursor/aluminum base pigment for **1** (c) and **2** (d), as determined by EDX. Each single point reflects 5 independent measurements with error bar.

can be observed, while at a value of 1 (Figure 6b) first surplus particle deposition occurred.

For precursor **2** the inhomogeneities during transformation into the oxide at a precursor/substrate ratio of 0.5 are still relatively small but start to increase rapidly at values of 0.7 and higher. SEM images for a ratio of 0.5 show that the coated pigments still possess homogeneous surfaces (Figure 6c). At a ratio of 1, however, the existence of massive precipitates in the range of several micrometers can be observed (Figure 6d). Hence, the development of smooth surfaces with no defects requires a slower coating speed with less amount of precursor **2** compared to the deposited oxide films derived from precursor **1**. This can be explained by faster decomposition kinetics of **2**, increasing the tendency to form inhomogeneous precipitates. However, the coating thicknesses obtained under such conditions are only a few nanometers, which is insufficient for obtaining the desired interference color changes. Therefore, the coating of the Al base pigment has to be at least 20–30 nm in thickness.[5] In order to make these discrete dimensions accessible, a sequential coating technique with periodical renewal of solvent was studied (Figure 6e). The effect observed is significant as the amount of side precipitation for sequentially coated pigments is much higher when the solvent is not exchanged during the process (Figure 6f). Therefore, ideal base pigment coatings could be obtained when (i) using low precursor/aluminum ratios, (ii) employing repetition of the coating process for several times and (iii) which are accompanied by a periodic exchange of the solvent to remove any side precipitates. This procedure is maintained until an observable change in the hue of the coated base pigments from silver to gold appears. An SEM image of the obtained optimized pigments from decomposition of **1** is shown in Figure 6g. The mean iron/aluminum ratio in the coated base pigments was determined to be 0.596 with a calculated standard deviation of 0.048, what is a relatively low value confirming the good homogeneity of the obtained coating. SEM images of obtained pigments using the optimized parameters for the decomposition of **2** are shown in Figure 6h. The mean copper/aluminum ratio is 0.569, the standard deviation is 0.134. This error is higher compared with the optimized coatings obtained from **1**, but is still much lower than the deviations using a non-optimized procedure for **2**.

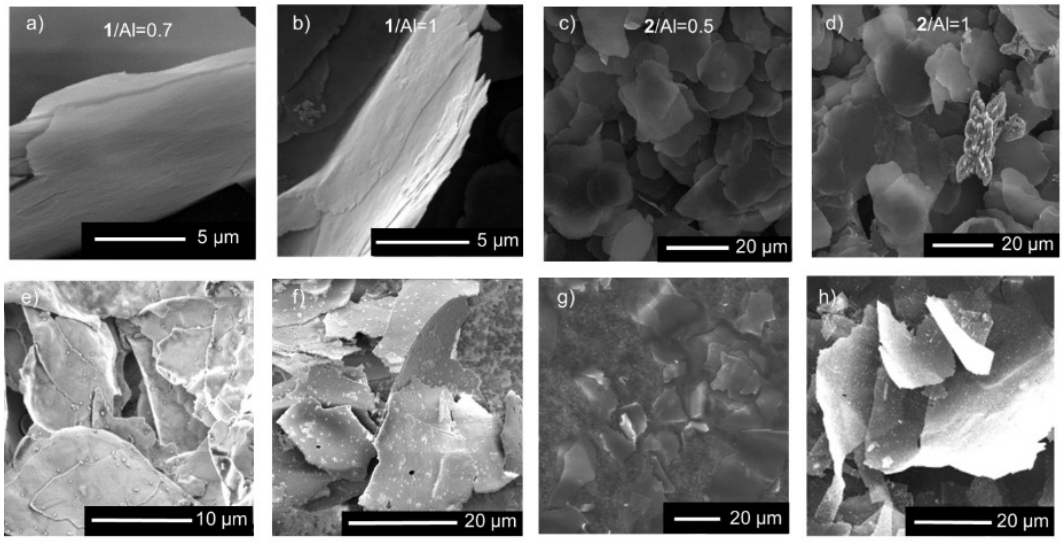

Figure 6. SEM images of coated Al base pigments obtained from **1** and the silverdollar base pigment with ratios of 0.7 (a), 1 (b), and from **2** and base pigment ratios of 0.5 (c) and 1 (d). Additionally, base pigments sequentially coated are shown in (e) with and in (f) without exchange of solvent and the pigments coated using the optimized procedure from decomposition of **1** (g) and **2** (h).

2.3. Spectroscopic Characterization of the Solution Precipitated Pigment Coatings

The results of the TG analysis reveal that the transformation of the precursor compounds **1** and **2** into the oxide coatings in solution is not complete under the chosen conditions (1-methoxy-2-propanol, 120 °C). The infrared spectrum of the product obtained from the thermal decomposition of the iron urea nitrate compound **1** in absence of aluminum base pigment is shown in Figure 7. The observed significant number of intense bands confirms the expected incomplete decomposition of the precursor. The signal at 1630 cm^{-1} has a far higher intensity than in urea. This can be assigned to either nitrate valence vibrations,[48–50] or vibration deformation modes originating from FeOOH (δ_{OH}, β-FeOOH).[51,52] The band at 1292 cm^{-1} corresponds solely to ν_s in NO_3.[49,50] Additional vibration modes at 1152 correspond to δ_{OH}, (γ-FeOOH), at 1013 to δ_{OH}, (γ-FeOOH) and at 890 and 790 cm^{-1} respectively, to δ_{OH} (α-FeOOH).[51–54] Additional bands at 1091 and at 1410 cm^{-1} have also been reported to be characteristic for α-Fe_2O_3[55] and FeOOH[51] or additional nitrate impurities.[52]

A thermogravimetric measurement of the oxide precipitate obtained from thermal decomposition of **1** in methoxypropanol (120 °C, 2 h) under oxygen atmosphere was performed in order to determine the quantity and nature of organic content in the obtained oxide material and to investigate its remaining decomposition under further thermal treatment (Figure 8a, black trace). The primary precipitate obviously undergoes a multi-step decomposition process. The first decomposition step confirms a slight mass loss of 3% in the temperature range from 100 to 140 °C, followed by a major mass loss of 30% from 140 to 265 °C. From 330 to 390 °C an increase of about 2% is observed which can be explained by the oxidation of the formed iron species. Between 390 °C up to 495 °C again a mass loss of about 11% is observed. The total mass loss observed during transformation of the solid obtained from the decomposition of **1** is 42%, indicating a massive organic residue under these conditions. The species comprising this residue can be concluded to mainly consist of undecomposed urea, as the observed mass vs. temperature profile (Figure 8a, black) is typical for the pyrolysis of urea.[46,47,56] In addition, the infrared spectrum reveals the presence of urea in the pyrolysis product from solution decomposition (Figure 7). Such a high organic content might influence the refractive index of the oxide pigment coating and therefore also the color saturation of the final coated pigment. To furthermore increase the purity of the coating layer, small amounts of water as oxidizing agent have been added to the precursor solution. As the thermogravimetric measurements show (Figure 8a), the presence of water in the precursor solution has a massive influence on the decomposition behavior, as the mass loss can be reduced by about 15% from 42% to 27% by addition of 1% H_2O. Additionally, the high temperature mass loss at 400 °C arising from polymerization reactions between isocyanic acid released during urea decomposition and still undecomposed urea disappears.[45–47] Water inhibits these reactions as it reacts with isocyanic acid under formation of evaporating NH_3 and CO_2.[47] In addition, even the formation of isocyanic acid is prevented as urea can be hydrolyzed directly to form ammonium carbonate, which decomposes immediately into ammonia and carbon dioxide.[44] These effects are detectable in the infrared spectrum of the precipitate (Figure 7). The intensity of the urea bands is reduced and the ammonia bands around 3300 cm^{-1} become slightly obstructed by an intense OH valence vibration. The intensities of the bands at 1659 and 1410 cm^{-1} attributable to FeOOH are increased. This signal increase, while the NH vibration at 1588 cm^{-1} is only existent as a weak signal, can also be

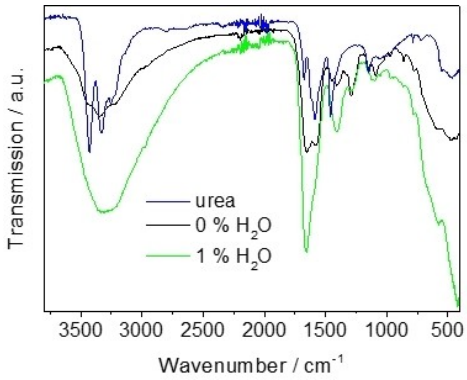

Figure 7. Infrared spectra of the precipitates obtained from refluxing **1** in 1-methoxy-2-propanol for 2 hours with no addition (black) and 1% (green) addition of H_2O.

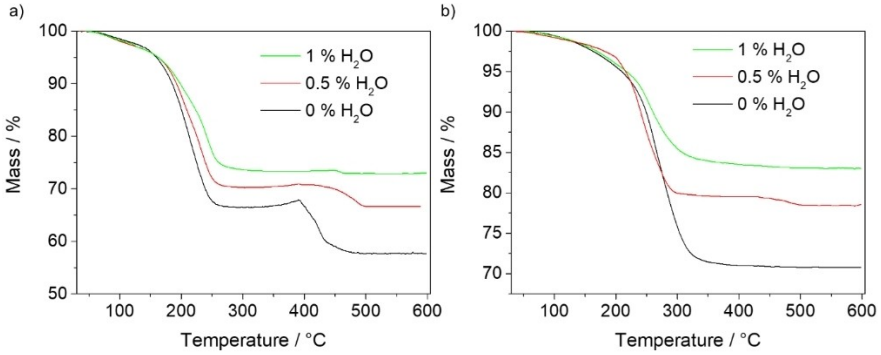

Figure 8. TG measurements of the obtained iron oxide precipitate under oxygen atmosphere obtained from refluxing of **1** in 1-methoxy-2-propanol for 2 hours with water content of 0% (black), 0.5% (red) and 1% (green) (a) and after following heat treatment in phenyl ether for 5 minutes at 259 °C (b).

attributed to carboxylates that were formed during urea hydrolysis. A further benefit of the reduction of organic residues by the addition of water is that no significant influence on the topography of the coatings formed on aluminum base pigments could be observed (S2). Removal of the remaining organic species accompanied by formation of hematite through calcination at 370 °C seems possible (S3). However, it is not suitable for the coated pigments as agglomeration occurs during such a heat treatment under ambient atmosphere (S4). That is why a solution-based approach was chosen to further reduce these impurities. Due to solvent interaction thermal processing at 259 °C for 5 minutes in phenyl ether leads only to minor particle aggregation when compared to a thermal annealing of the solid (S4). The organic content could thus be massively reduced. The thermogravimetric measurements of the precipitate obtained after refluxing in phenyl ether without addition of water (Figure 8b) reveal a reduced mass loss of 12% (from 42% to 30%) and for the precipitate obtained after addition of 1% water of 10% (from 27% to 17%). The latter is the lowest value for the obtained iron species. However, a major effect is already seen for a sample obtained after usage of 0.5% water with a mass loss of 22%. As it is also desired to use as low water as possible to avoid oxidation of the aluminum base pigment, a reduced water content of 0.5% is supposed to be the optimum in regard of the overall performance. Figure 10a shows an XRD of a base pigment coated under these optimal conditions, revealing that the temperature is high enough to observe a beginning crystallization of γ-Fe_2O_3 (JCPDS card no. 25-1402) maghemite, with broad reflexes visible at 35

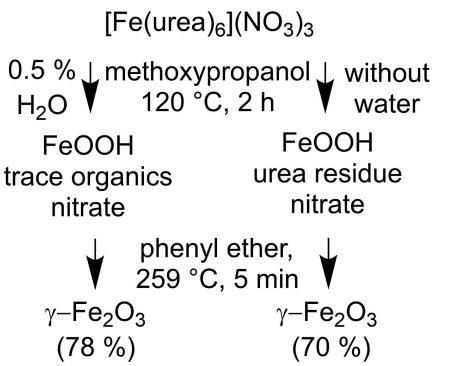

Figure 9. Scheme of the processes described herein starting from 1.

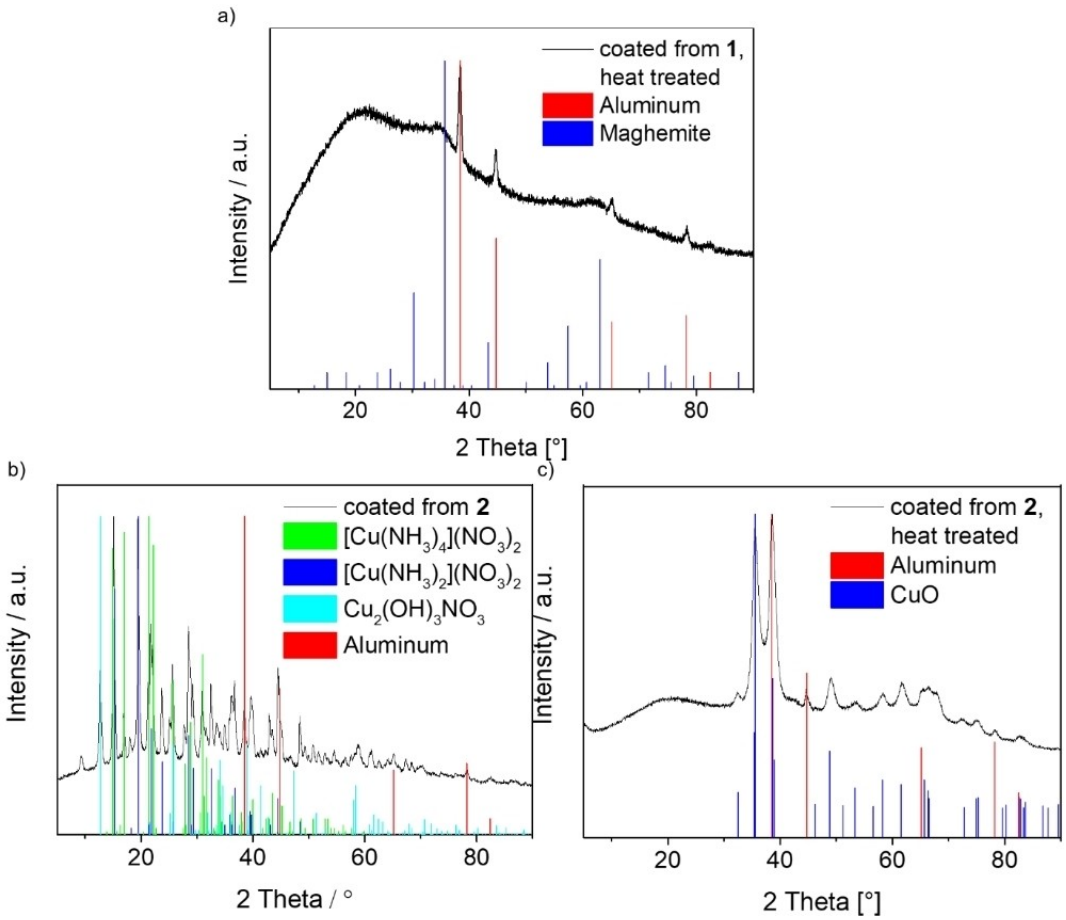

Figure 10. XRD analysis of the base pigments (a) coated by thermal decomposition of **1** and heat treatment in phenyl ether compared with metallic aluminum (red)(JCPDS 04-0787) and maghemite (blue)(JCPDS 25-1402), (b) coated by thermal decomposition of **2** in 1-methoxy-2-propanol, 120 °C, 2 h, compared with tetraamminecopper(II) nitrate (green)(JCPDS 51-0271), diaminecopper(II) nitrate (blue) (JCPDS 48-1187), copper nitrate hydroxide (cyan)(COD 9012715) and aluminum (red)(JCPDS 04–0787). (c) coated starting from 2 and heat treated in phenyl ether compared with metallic aluminum (red)(JCPDS 04-0787) and CuO (blue)(JCPDS 80-0076).

and 63 °2θ besides reflexes of the aluminum substrate (JCPDS card no. 04-0787).

The oxidizing step and the high temperature mass loss around 400 °C disappear after treatment in phenyl ether no matter if water had been used during the precipitation in 1-methoxy-2-propanol. We speculate that during heat treatment, FeOOH is transformed into iron oxide accompanied by release of water. Under ambient atmosphere, water evaporates immediately, and urea decomposes under formation of larger molecules with higher thermal stability like cyanuric acid, ammelide, ammeline and melamine.[45–47] In solution however, water could stay in the solvent medium for a longer time, thereby leading to the positive effects described afore. With increasing water content in the initial precursor solution, the content of FeOOH rises thereby increasing this effect and reducing the final mass. A summary of the transformation processes, proven intermediates and final products is presented in Figure 9.

While **1** shows incomplete decomposition in solution (Figure 9) and urea remains intact to a large extent, in the case of **2** decomposition of the urea and formation of ammonia complexes can be observed (Figure 12). XRD analysis of the decomposition product of **2** reveals several products after refluxing a solution containing **2** for two hours (Figure 10b). Besides signals originating from the aluminum base pigments, the existence of mainly tetraamminecopper(II)nitrate (JCPDS card no. 51-0271) and diamminecopper(II)nitrate (JCPDS card no. 48-1187) is confirmed. Some additional small reflexes cannot be assigned in detail but are most likely to belong to some additional amine/hydroxo/nitrate phases. The mass loss measured by TG for the copper precipitate in absence of aluminum is 67.6% (Figure 11), lying between the expected values for $[Cu(NH_3)_2](NO_3)_2$ (64.1%) and $[Cu(NH_3)_4](NO_3)_2$ (68.9%), so that the amino nitrates can be regarded as the dominant transformation products. As heat treatment in solution already showed promising results during the processing of the coated base pigments obtained from **1**, this approach was also further studied for the coated base pigments using precursor **2**. The TG studies (Figure 11) reveal that the mass loss after heat treatment is reduced drastically from 64.3 to 12.0%, showing that most of the organic species could be eliminated using this process. Besides the aluminum phase of the base pigment the formation of crystalline CuO (JCPDS card no. 80-0076) is detected (Figure 10c).

In conclusion, compound **2** shows an advantageous decomposition behavior in solution as compared to **1**. The energetic driving force for the decomposition of the precursors is formation of the amino nitrate complexes, which are unstable under heat treatment and tend to decompose vigorously.[57] These are not existent with iron as cation, which is why urea still remains intact to a large extent after decomposition of **1**. Another positive aspect of the copper coated pigments is that only minor particle agglomeration can be observed during the process (S4).

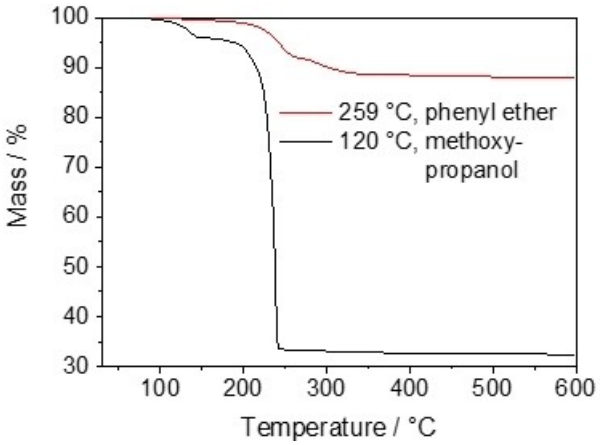

Figure 11. Thermogravimetric measurements under oxygen atmosphere of the oxide precipitates obtained from refluxing **2** in 1-methoxy-2-propanol for 2 hours (black) and after following treatment in phenyl ether for 5 minutes at 259 °C (red).

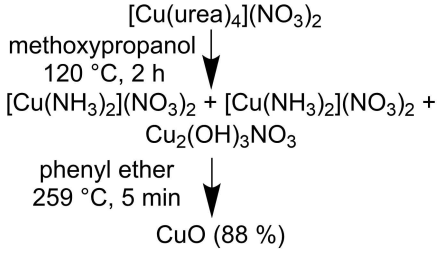

Figure 12. Scheme of the processes described herein starting from **2**, leading to copper oxide with a purity of 88%.

2.4. Colorimetric Investigations of the Final Iron Oxide and Copper Oxide Coated Aluminum Base Pigments

Table 1 provides an overview over the pigments investigated herein, which are the commercial coated aluminum based pigments Paliocrom® Brilliant Gold L 2050 ("Palio" a silverdollar-type Al base pigment coated with Fe_2O_3 using a fluidized bed

Table 1. Overview over the metal oxide coated pigments investigated in this work. Shown are the type of Al base pigments, short processing information corresponding to the sample names used. Degree of pigmentation of the investigated varnishes containing the commercial pigments was 7% and the pigments synthesized herein 3%.

Sample name	Pigment type	Fabrication
Palio	Silver dollar	Paliocrom®; coated with Fe_2O_3 in a fluidized bed reactor
Ale	PVD	Alegrace®; wet chemically coated with SiO_2 and Fe_2O_3
1-nopt	PVD	thermal decomposition of **1**, not optimized procedure without solvent exchange during the coating steps
1-nopt-calc	PVD	thermal decomposition of **1**, not optimized procedure; heat treated in phenyl ether
1-opt	PVD	thermal decomposition of **1**, optimized procedure with solvent exchange during the coating steps
1-opt-DPE	PVD	thermal decomposition of **1**, optimized procedure, heat treated in phenyl ether
2-opt-DPE	PVD	thermal decomposition of **2**, heat treated in phenyl ether

reactor) and Alegrace® Aurous A 21/71-1 White Gold ("Ale" a PVD Al base pigment, wet chemically coated with SiO_2 and Fe_2O_3). The herein synthesized pigments are coated Decomet® pigments obtained from decomposition of **1** using (i) an unoptimized procedure without exchange of solvent (**1**-nopt), (ii) calcined at 400 °C for 4 h under ambient atmosphere (**1**-nopt-calc), (iii) using the optimized procedure (**1**-opt) and finally (iv) an optimized pigment (**1**-opt) which is additionally heat treated in phenyl ether (**1**-opt-DPE) employing the strategies described before. Moreover, the copper oxide coated Al base pigments (**2**-opt-DPE) were obtained from decomposition of **2** followed by additional heat treatment in phenyl ether (see table 1).

The corresponding optical spectra (S5-9) and a table with the numeric values of the optical parameters (S10) derived from the spectra are given in the supplementary information. Figure 13 shows a comparison of the characteristic coloristic values for the differently coated aluminum base pigments (see table 1). Gloss describes the intensity of the reflectance of the material from the glancing angle. The color saturation S is important for the optical performance of a pigment, as it relates the chromaticity and the lightness. If the saturation is high, the color of the material looks intense, while it appears pale for lower values. The flop index is a measure for the change of the optical appearance of a sample when observed from different viewing angles.

The color distance dE describes the distance of two samples in the CIELAB color space.[58,59] Here, it is used to determine the hiding power, as the same sample is measured on a black and a white background. When the hiding power is high, the dE should be close to 0, meaning that the underground is optimally covered by the pigments. In the case of a weak hiding power the influence of the underlying background becomes dominant and dE rises.[58,60,61]

For the coloristic investigations, all pigments were dispersed in a varnish and deposited on a black/white card by doctor blading technique. A comparison of the not optimised pigments obtained without exchange of solvent during the coating steps (**1**-nopt), and the same pigments calcined at 400 °C (**1**-nopt-calc), shows that the color saturation reaches the highest values of all pigments synthesized in this work after calcination (Figure 13a). This can be attributed to the most complete removal of organic residues originating from the precursor molecule **1** and almost complete oxidation of the iron species. However, the coloristic measures as gloss, flop index and hiding power are drastically diminished (Figure 13b–d). This can be attributed to the observed particle agglomeration (S3) which hinders a homogeneous distribution of the pigments in the deposited film while increasing the inhomogeneity of the

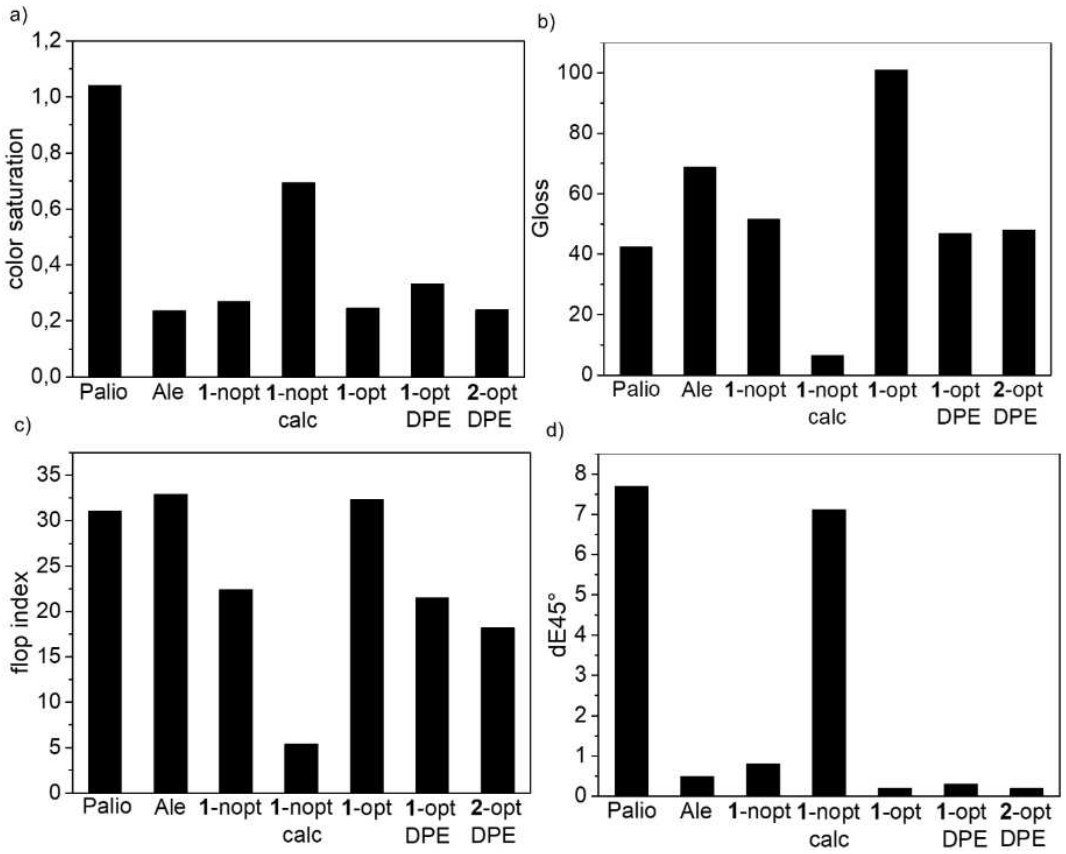

Figure 13. Comparison of the colorimetric results of the obtained pigments at different stages of the process compared with Paliocrom® Brilliant Gold L 2050 ("Palio") and Alegrace® Aurous A 21/71-1 White Gold ("Ale"). Bold numbers indicate the complex used for the precipitation. Shown are results for color saturation (a), gloss (b), flop index (c) and the color distance dE45° between black and white background from 45° (d).

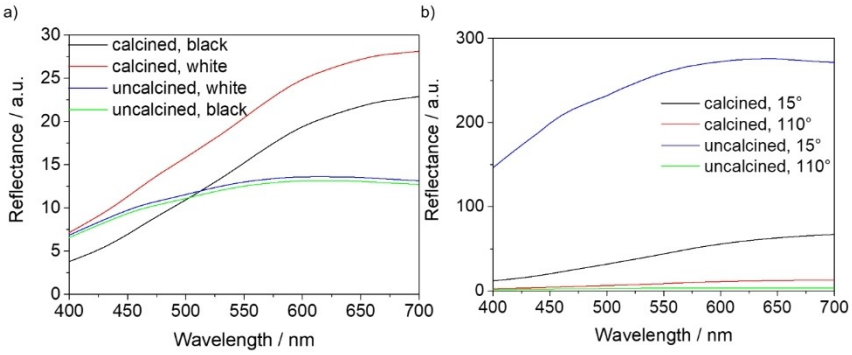

Figure 14. Optical reflectance spectra of pigment samples coated by thermal decomposition of **1**; a) from 45°, shown are the calcined (400 °C, 4 h) sample on white (red trace) and black (black trace) background and the uncalcined pigment sample on white (blue trace) and black (green trace) background; b) shows spectra on black background of the calcined sample from 15° (black trace) and 110° (red) and for the uncalcined sample from 15° (blue trace) and 110° (green trace).

coated pigments which causes an increased diffuse reflectivity in the particles and can obviously only be obtained when the pigment is nicely dispersed. Figure 14a, shows the spectra of the samples before and after ambient calcination. An optimal hiding power is characterized by a low color distance between the pigments measured on a black and a white background from a viewing angle of 45°. The dE45° should be ideally below 1. The spectra of the uncalcined sample show nearly the same habitus, while in the case of the calcined samples a relatively large difference can be observed. In addition, the flop decreases drastically after calcination. This value depends mainly on the difference between the lightness at 15° and 110°; the bigger the difference the higher is the flop. The spectra of the samples before and after ambient calcination on a black background measured from an angle of 15° and 110° reveal that the difference in the spectra of the sample before calcination is significantly higher than after heat treatment (Figure 14b).

The photos of the obtained pigments dispersed in a varnish visualize the effects of the different treatments. It can be clearly seen that the gloss of the sample calcined at 400 °C (Figure 15b) is much lower than the values of the others, which possess extremely high glance. On the other hand, the 400 °C calcined sample has by far the best color saturation; all the other varnishes appear comparatively pale. A small improvement of the color saturation can be observed after treatment in phenyl ether (Figure 15d) due to the lowered content of organic residues (Figure 8). However, a drawback are the reduced gloss and flop index, which can be attributed to changes in the surface morphology of the varnish. After precipitation of the coatings at 120 °C, the organic residues are most likely to be evenly distributed in the deposited film. During heat treatment, these residues evaporate, leaving micro voids in the surface. In addition, the oxidic phases start to contract during a beginning crystallization process. SEM images show indeed a reduced homogeneity after heat treatment (Figure 16b). This observed inhomogeneity results in a lowered gloss and flop of the CuO-coated pigments (Figure 16c), while the surface of the Fe_2O_3-coated pigments appears significantly smoother (Figure 16d). However, both Al base pigments show dense and homogeneous oxide coatings with no visible macroscopic cracks.

Compared with the two commercial aluminum base pigments Paliochrom® and Alegrace®, all pigments synthesized herein, except the one calcined in ambient atmosphere, show

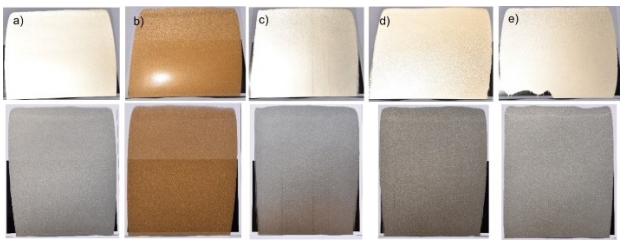

Figure 15. Photos of the varnish pigments applied on a cardboard with black and a white background. The pigments are deposited by the doctor blading technique. The cardboards are viewed from the glancing angle (top line) and directly from above (bottom line); a, **1**-nopt; b, **1**-nopt-calc; c, **1**-opt; d, **1**-opt-DPE; e, **2**-opt-DPE.

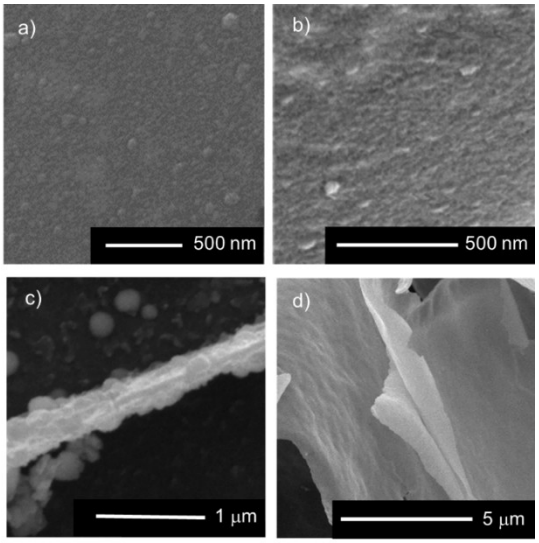

Figure 16. SEM images of the surfaces of the coated pigments obtained from precipitation of **1** before (a) and after (b) treatment in phenyl ether at 259 °C, 5 min. Lateral view of the CuO-coated (c) and Fe_2O_3-coated (d) pigments.

similar or even higher gloss values, indicating that they match or outperform the state of the art. However, due to the remaining organic residues, the samples appear comparably pale. A further major advantage of the samples can be observed as far as the hiding power is concerned. The pigments synthesized herein show a much better hiding strength compared to the state-of-the-art pigments (Figure 13). Although the degree of pigmentation in the formulation is only 3%, the pigment sample synthesized from precursor compound **1** before calcination under optimized conditions has a dE45° of only 0.2. For Paliocrom® Brilliant Gold L 2050 it is 7.7 even at a higher degree of pigmentation of 7%. For a material with a sufficiently good hiding power, a dE45° value of not more than 1 is desirable. The reason for the extraordinary hiding power may be due to the optimized coating process using the molecular precursors **1** and **2** which allows a smooth deposition of the molecular precursor followed by a transformation into the oxidic pigments. This allows a very narrow and smooth coverage of the ultrathin physical vapor deposited aluminum base pigments. It is known that the thinner a base pigment is, the lower is the amount needed for a hiding coverage in a varnish.[27]

3. Conclusions

A solution based environmentally benign procedure for coating of aluminum metal effect pigments using a single source precursor route is presented. It was possible to synthesize special effect pigments based on ultrathin physical vapor deposited aluminum flakes (Decomet®). All reagents used herein are safe to handle, nontoxic, environmentally friendly and allow an uncomplicated adaptation towards technological scale up. Due to the single source precursor approach the reaction control is straightforward as the metal oxide source, oxidizing agent and fuel for the combustion reaction are combined in one molecular compound. Interestingly, the iron precursor for the iron oxide coating is also available in a direct approach using iron metal and urea. Because of the versatility of the urea ligand in coordination chemistry the single source precursor approach offers access to a wide variety of other metal oxides, too.[40] The synthesized pigment coatings show a homogeneous surface leading to excellent coloristic values for gloss (45–100) and flop indices (20–30). The color saturation is comparatively weak (0.2–0.3), probably due to minor amounts of residual organics still remaining in the film (~15%). Solid state calcination in ambient atmosphere is challenging due to particle agglomeration during oxide film formation. However, it was possible to largely reduce the content of organic impurities by heat treatment in solution. It was possible to coat aluminum base pigments directly without application of a protective layer as it is needed in the currently commercially established sol-gel coating procedures to avoid pigment decomposition. The coated aluminum base pigments show an excellent hiding power exceeding that obtained in current state of the art pigments by far with dE45° of only ~0.3 for varnishes with a low degree of deposited pigment of only 3%. This drastically reduced material demand in automobile paint lacquers could lead to significant saving of costs and contributes to a protection of the environment.

Experimental Section

Materials

Iron(III) nitrate nonahydrate, ethanol and 1-butanol were purchased from VWR, copper(II) nitrate trihydrate and 1-Methoxy-2-Propanol from Roth, urea and phenyl ether from Merck. Alustar®, Decomet® and Alegrace® Aurous A 21/71-1 White Gold were obtained from Schlenk Metallic Pigments GmbH and Paliocrom® Brilliant Gold L 2050 from BASF.

Precursor Synthesis

Hexakis(urea)iron(III)nitrate (**1**) was synthesized according to a literature procedure[43]: Iron nitrate nonahydrate (4.85 g, 12 mmol) was dissolved in 250 mL EtOH and urea (6.006 g, 100 mmol) was dissolved in 100 mL ethanol. Both solutions were mixed and stirred for 2 hours. The precipitation of a yellow product was observed, which was separated by filtration, washed in ethanol, and dried in vacuo (5.29 g, 73%). Anal. Calcd (%) for $C_6H_{24}FeN_{15}O_{15}$ (601.8 $gmol^{-1}$) C 11.97 H 3.99 N 34.92; found C 12.40 H 3.93 N 35.46. TG ceramic yield (%) Calcd 13.26, found 13.77. ^{1}H NMR ([D_6] dimethyl sulfoxide, 25 °C) δ = 5.43 ppm (br, NH_2). IR $\tilde{\upsilon}$ = 3437 (s, $\nu_{NH,\ in\ phase}$), 3339 (s, $\nu_{NH,\ in\ phase}$), 3233 (s, $\nu_{NH,\ in\ phase}$), 1625 (s, ν_{CO}), 1551 (s, δ_{NH}), 1504 (s, ν_{CN}), 1332 (s, ν_{NO}), 1148 (m, ρ_{NH}), 1031 (m, ρ_{NH}), 828 (w, ω_{NH}), 760 (w, ω_{NH}), 609 (m, δ_{CN}), 537 (m, δ_{CN}), 429 (m, δ_{CN}).

In an alternative approach, **1** was synthesized directly from iron metal. Iron powder (0.089 g, 1.6 mmol) was dispersed in 5 mL ethanol and 308 µL nitric acid (65%) added. After stirring for 1 day, unsolved iron was removed. Additionally, 0.59 g urea (9.8 mmol) was dissolved in 20 mL ethanol. Both solutions were mixed and stirred for 2 hours. The resulting yellow precipitate was separated by filtration, washed in ethanol, and dried in vacuo (0.364 g, 38%). Anal. Calcd (%) for $C_6H_{24}FeN_{15}O_{15}$ (601.8 $gmol^{-1}$) C 11.97 H 3.99 N 34.92; found C 11.63 H 4.74 N 34.46. TG ceramic yield (%) Calcd 13.26, found 13.45. ^{1}H NMR ([D_6] dimethyl sulfoxide, 25 °C) δ = 5.39 ppm (br, NH_2). IR $\tilde{\upsilon}$ = 3436 (s, $\nu_{NH,\ in\ phase}$), 3335 (s, $\nu_{NH,\ in\ phase}$), 3225 (s, $\nu_{NH,\ in\ phase}$), 1625 (s, ν_{CO}), 1549 (s, δ_{NH}), 1501 (s, ν_{CN}), 1331 (s, ν_{NO}), 1148 (m, ρ_{NH}), 1030 (m, ρ_{NH}), 828 (w, ω_{NH}), 759 (w, ω_{NH}), 610 (m, δ_{CN}), 538 (m, δ_{CN}), 424 (m, δ_{CN}).

Tetrakis(urea)copper(II)nitrate (**2**) was synthesized according to a literature procedure with small adaptations[62]: Urea (5 g, 83.3 mmol) was dissolved in 300 mL *n*-butanol at 50 °C. After complete dissolution, copper nitrate trihydrate (4.82 g, 20.0 mmol) was added and the mixture stirred for 2 hours. The resulting blue precipitate was separated by filtration, washed with n-butanol and 2-Propanol and dried in vacuo (6.33 g, 74%). Anal. Calcd (%) for $C_4H_{16}CuN_{10}O_{10}$ (427.8 $gmol^{-1}$) C 11.22 H 3.74 N 33.25; found C 11.87 H 3.74 N 32.74. TG ceramic yield (%) Calcd 18.59, found 18.68. ^{1}H NMR ([D_6] dimethyl sulfoxide, 25 °C) δ = 6.16 ppm (br, NH_2). IR $\tilde{\upsilon}$ = 3470 (s, $\nu_{NH,\ in\ phase}$), 3400 (s, $\nu_{NH,\ in\ phase}$), 3335 (s, $\nu_{NH,\ in\ phase}$), 3233 (s, $\nu_{NH,\ in\ phase}$), 1621 (s, ν_{CO}), 1567 (s, δ_{NH}), 1508 (s, ν_{CN}), 1385 (s, ν_{NO}), 1329 (s, ν_{NO}), 1151 (m, ρ_{NH}), 1053 (m, ρ_{NH}), 1028 (m, ρ_{NH}), 815 (w, ω_{NH}), 757 (w, ω_{NH}), 608 (m, δ_{CN}), 540 (m, δ_{CN}), 426 (m, δ_{CN}).

Pigment Coating

For the process optimization, the silverdollar-type aluminum base pigment Alustar® (thickness 150–300 nm) supplied by Schlenk Metallic Pigments GmbH was used. In the general coating procedure, the aluminum base pigment was dispersed in 1-methoxy-2-propanol. The precursor compound **1** or **2** was added in the desired ratio and the mixtures refluxed (120 °C) for 2 hours. For the investigation of the coating materials alone, the whole procedure was done in the same way in absence of aluminum pigments. For the final samples for the coloristic investigations the physical vapor deposited aluminum base pigment Decomet® (thickness 1–50 nm) supplied by Schlenk Metallic Pigments GmbH was used. The synthesis conditions of the coated pigments investigated there are as follows:

1-nopt: 1 g of the pigment paste was dispersed in a mixture of 100 mL 1-methoxy-2-propanol and 1 mL water. 1 g **1** was dissolved therein and refluxed for 2 hours. After cooling down, 1 more g **1** was added and again refluxed for 2 hours. The process was repeated one more time. The resulting coated substrates were isolated by filtration, washed with isopropanol and dried for 16 hours at 50 °C.

1-nopt-calc: The sample was synthesized in the same way as **1**-nopt, but in the end additionally calcined at ambient atmosphere in a muffle furnace at 400 °C for 4 h.

1-opt: 1 g of the Decomet® paste was dispersed in a mixture of 100 mL 1-methoxy-2-propanol and 0.5 mL water and coated in 6 steps consisting of addition of 0.5 g **1** and refluxing for 2 h. After each second step, the solvent was renewed. The resulting pigments were filtered off, separated by filtration, washed in isopropanol and redispersed in isopropanol.

1-opt-DPE: The sample was synthesized under the same conditions as **1**-opt following heat treatment in phenyl ether (259 °C, 5 minutes). The resulting pigments were separated by filtration, washed in ethanol, acetone and diethyl ether and redispersed in isopropanol.

2-opt-DPE: 1 g Decomet® was dispersed in 100 mL 1-methoxy-2-propanol and coated in 8 steps, consisting of refluxing for 2 h with varying amounts of **2** (0.2 g for step 1 + 2, 0.3 g for step 3 + 4, 0.5 g for step 5–8). After step 4 the solvent was renewed. Thereafter the coated substrates were filtered off, redispersed in phenyl ether and refluxed for 5 min. The resulting pigments were filtered off, separated by filtration, washed in isopropanol and dried at 50 °C for 16 hours.

Two commercial Fe_2O_3 coated aluminum pigments were used for comparison of the coloristic values. Paliocrom® Brilliant Gold L 2050 is a silverdollar-type aluminum base pigment coated with iron oxide from BASF using a fluidized bed reactor. Alegrace® Aurous A 21/71-1 White Gold is a physical vapor deposited aluminum base pigment wet chemically coated with SiO_2 and Fe_2O_3 supplied by Schlenk Metallic Pigments GmbH.

Material Characterization

The XRD data were collected using a Rigaku Miniflex 600@40 kV 15 mA diffractometer with $Cu_{k\alpha 1}$ radiation ($\lambda = 1.541$ Å). IR spectra were collected with a Nicolet 6700 (ThermoScientific). SEM images were taken using XL30 FEG by Philips coupled with genesis X4 M (EDAX) for EDX measurements with the samples fixed on a carbon tape. The sample was measured at 5 different spots and a medium value calculated. The samples were sputtered with 3 nm Pt/Pd (80/20) using a Cressington 208 HR Sputter Coater. The particle sizes were determined by static light scattering in a Saturn DigiSizer II 5205 (Micromeritics) with isopropanol as solvent. TG measurements were performed using a 209-Iris (Netzsch) coupled with a QMS 403 C mass spectrometer (Netzsch) and an infrared spectrometer Nicolet iS10 (ThermoScientific) under oxygen atmosphere using aluminum crucibles. For the colorimetric investigations, the pigments were dispersed in a nitrocellulose/polycyclohexanone/polyacrylic varnish and applied on a black/white DIN A5 card (TQC) using an automatic system from Zehntner with a 38 µm spiral blade. The coloristic values were measured using the device Byk-mac i (Byk) except the gloss, which was determined with the system Byk micro-TRI-gloss (Byk). The illumination spectrum used was D65 norm light.

Acknowledgements

Support through the Technical University of Darmstadt is acknowledged with gratitude. We gratefully acknowledge F. Burger (Schlenk Metallic Pigments GmbH) for the coloristic measurements and S. Heinschke (TUDa) for performing XRD measurements.

Conflict of Interest

The authors declare no conflict of interest.

Keywords: copper · iron · metal oxide thin films · special effect pigments · urea-nitrate compounds

[1] R. R. Holloway, *Am. J. Archaeol.* **2006**, *110*, 365.
[2] S. Sotiropoulou, D. Sister, *Acc. Chem. Res.* **2010**, *43*, 877.
[3] D. A. Scott, *Stud. Conserv.* **2016**, *61*, 185.
[4] F. J. Maile, G. Pfaff, P. Reynders, *Prog. Org. Coat.* **2005**, *54*, 150.
[5] G. Pfaff, *Spezielle Effektpigmente. Grundlagen und Anwendungen*, Vincentz Network, Hannover, **2007**.
[6] Thomas Schlegl, Stefan Trummer, Frank Henglein, Ralph Schneider, Thomas Schuster (Eckart GmbH & Co., KG), US 2007/0199478 A1, **2007**.
[7] Kaiman Shimizu, Fabian Piech, Adalbert Huber (Schlenk Metallic Pigments GmbH), EP3053967 A1, **2014**
[8] Gerhard Pfaff, *Inorganic Pigments*, de Gruyter, Berlin/Boston, **2017**.
[9] Q. Gao, X. Wu, Y. Fan, X. Zhou, *Dyes Pigm.* **2012**, *95*, 534.
[10] G. Pfaff, *Inorg. Mater.* **2003**, *39*, 123.
[11] L. Skowronski, A. A. Wachowiak, W. Wachowiak, *Appl. Surf. Sci.* **2017**, *421*, 794.
[12] S. A. Hassanzadeh-Tabrizi, *J. Coat. Technol. Res.* **2015**, *12*, 751.
[13] R. Maisch, O. Stahlecker, M. Kieser, *Prog. Org. Coat.* **1996**, *27*, 145.
[14] H. Du, C. Liu, J. Sun, Q. Chen, *Powder Technol.* **2008**, *185*, 291.
[15] C. Jing, S. X. Hanbing, *Dyes Pigm.* **2007**, *75*, 766.
[16] M. Ren, H. Yin, C. Ge, J. Huo, X. Li, A. Wang, L. Yu, T. Jiang, Z. Wu, *Appl. Surf. Sci.* **2012**, *258*, 2667.
[17] Y. Zhang, H. Ye, H. Liu, K. Han, *Powder Technol.* **2012**, *229*, 206.
[18] G. B. Smith, A. Gentle, P. D. Swift, A. Earp, N. Mronga, *Sol. Energy Mater. Sol. Cells* **2003**, *79*, 179.
[19] C. Schmidt, K. R. Bischoff, H. Bernius (Merck Patent GmbH), EP1595921 A1, **2005**
[20] S. Andes, S. George, M. Herbski, P. Reynders, R. Vogt, J. Dietz (Merck Patent GmbH), DE19836810 A1, **1998**
[21] J.-P. Jolivet, C. Chanéac, E. Tronc, *Chem. Commun.* **2004**, 481.
[22] C. Janiak, E. Riedel, *Anorganische Chemie (De Gruyter Studium)*, de Gruyter, **2011.**
[23] R. Supplit, U. Schubert, *Corros. Sci.* **2007**, *49*, 3325.
[24] Y. Zhang, H. Ye, H. Liu, K. Han, *Corros. Sci.* **2011**, *53*, 1694.
[25] L. Li, P. Pi, X. Wen, J. Cheng, Z. Yang, *Corros. Sci.* **2008**, *50*, 795.
[26] A. Kiehl, K. Greiwe, *Prog. Org. Coat.* **1999**, *37*, 179.

[27] B. Sarkodie, C. Acheampong, B. Asinyo, X. Zhang, B. Tawiah, *Color Res. Appl.* **2019**, *44*, 396.
[28] M. Legodie, D. Dewaal, *Dyes Pigm.* **2007**, *74*, 161.
[29] W. Ostertag, K. Bittler, G. Bock (BASF AG), EP0033457A2, **1981**.
[30] National Academies Press (US), Acute Exposure Guideline Levels for Selected Airborne Chemicals: Volume 6, Washington (DC), **2008**.
[31] S. Sanctis, R. C. Hoffmann, N. Koslowski, S. Foro, M. Bruns, J. J. Schneider, *Chem. Asian J.* **2018**, *13*, 3912.
[32] X. Yu, J. Smith, N. Zhou, L. Zeng, P. Guo, Y. Xia, A. Alvarez, S. Aghion, H. Lin, J. Yu et al., *Proc. Natl. Acad. Sci. USA* **2015**, *112*, 3217.
[33] L. Liu, G. Wu, W. Chen, Z. Xiong, T. He, P. Chen, *Int. J. Hydrogen Energy* **2015**, *40*, 429.
[34] J. P. R. Villiers, J. C. A. Boeyens, *J. Cryst. Mol. Struct.* **1975**, *5*, 215.
[35] P. C. Srivastava, B. N. Singh, C. Aravindakshan, K. C. Banerji, *Thermochim. Acta* **1983**, *71*, 227.
[36] R. Keuleers, J. Janssens, H. O. Desseyn, *Thermochim. Acta* **2000**, *354*, 125.
[37] D. S. Sagatys, R. C. Bott, G. Smith, K. A. Byriel, C. H. L. Kennard, *Polyhedron* **1992**, *11*, 49.
[38] L. Drakopoulou, C. Papatriantafyllopoulou, A. Terzis, S. P. Perlepes, E. Manessi-Zoupa, G. S. Papaefstathiou, *Bioinorg. Chem. Appl.* **2007**, 51567.
[39] P. Sharma, J. Bhale, A. Mishra, P. Malviya, *J. Phys. Conf. Ser.* **2014**, *534*, 12044.
[40] Theophile Theophanides, *Coord. Chem. Rev.* **1987**, *76*, 237.
[41] M. S. Lupin, G. E. Peters, *Thermochim. Acta* **1984**, *73*, 79.
[42] R. B. Penland, S. Mizushima, C. Curran, J. V. Quagliano, *J. Am. Chem. Soc.* **1957**, *79*, 1575.
[43] S. Zhao, H. Y. Wu, L. Song, O. Tegus, S. Asuha, *J. Mater. Sci.* **2009**, *44*, 926.
[44] O Carp, L Patron, L Diamandescu, A. Reller, *Thermochim. Acta* **2002**, *390*, 169.
[45] S. Désilets, P. Brousseau, D. Chamberland, S. Singh, H. Feng, R. Turcotte, K. Armstrong, J. Anderson, *Thermochim. Acta* **2011**, *521*, 59.
[46] P. M. Schaber, J. Colson, S. Higgins, D. Thielen, B. Anspach, J. Brauer, *Thermochim. Acta* **2004**, *424*, 131.
[47] D. Wang, S. Hui, C. Liu, *Fuel* **2017**, *207*, 268.
[48] M. Hesse, H. Meier, B. Zeeh, S. A. Bienz, L. Bigler, T. Fox, *Spektroskopische Methoden in der organischen Chemie*, Georg Thieme Verlag, Stuttgart, New York, **2012**.
[49] D. N. Sathyanarayana, *Vibrational spectroscopy. Theory and applications*, New Age International, New Delhi, **2004**.
[50] G. Socrates, *Infrared and Raman characteristic group frequencies. Tables and charts*, Wiley, Chichester, **2010**.
[51] F. Geng, Z. Zhao, J. Geng, H. Cong, H.-M. Cheng, *Mater. Lett.* **2007**, *61*, 4794.
[52] R. M. Cornell, U. Schwertmann, *The Iron Oxides. Structure, Properties, Reactions, Occurences and Uses*, Wiley-VCH, Weinheim, **2003**.
[53] D. G. Lewis, V. C. Farmer, *Clay Miner.* **1986**, *21*, 93.
[54] G. Nauer, P. Strecha, N. Brinda-Konopik, G. Liptay, *J. Therm. Anal.* **1985**, *30*, 813.
[55] B. Pal, M. Sharon, *Thin Solid Films* **2000**, *379*, 83.
[56] S. Désilets, P. Brousseau, D. Chamberland, S. Singh, H. Feng, R. Turcotte, J. Anderson, *Thermochim. Acta* **2011**, *521*, 176.
[57] T. M. Southern, W. W. Wendlandt, *J. Inorg. Nucl. Chem.* **1970**, *32*, 3783.
[58] H. G. Völz, *Industrielle Farbprüfung. Grundlagen und Methoden ; farbmetrische Testverfahren für Farbmittel in Medien*, VCH, Weinheim, **1990**.
[59] Ł. Skowroński, A. J. Antończak, M. Trzcinski, Ł. Łazarek, T. Hiller, A. Bukaluk, A. A. Wronkowska, *Appl. Surf. Sci.* **2014**, *304*, 107.
[60] G. Buxbaum (Ed.) *Industrial inorganic pigments*, Wiley-VCH, Weinheim [etc.], **1998**.
[61] W. Herbst, K. Hunger, *Industrial Organic Pigments*, Wiley-VCH, Hoboken, **2006**.
[62] M. Koman, E. Jona, D. Nagy, *Z. Kristallogr.-Cryst. Mater.* **1995**, *210*.

Manuscript received: August 11, 2020
Revised manuscript received: November 4, 2020